

# Lattice QCD predictions for shapes of event distributions along the freezeout curve in heavy-ion collisions

R. V. Gavai\* and Sourendu Gupta†

*Department of Theoretical Physics,  
Tata Institute of Fundamental Research,  
Homi Bhabha Road, Mumbai 400005, India.*

We present lattice QCD results along the freezeout curve of heavy-ion collisions. The variance, skew and kurtosis of the event distribution of baryon number are studied through Padé resummations. We predict smooth behaviour of three ratios of these quantities at current RHIC and future LHC energies. Deviations from this at lower energies signal the presence of a nearby critical point.

PACS numbers: 12.38.Gc, 25.75.-q, 11.15.Ha, 05.70.Fh

All matter that we know undergoes phase transitions as external conditions change. Strongly interacting matter, described by QCD, is not thought to be exceptional. Although the phase diagram of QCD matter is not yet established, it has been the subject of intense theoretical and experimental scrutiny in recent years. Finding a critical point in this system would be major landmark. One idea is to look at quantities which are non-monotonic near a critical point. In this letter we give lattice predictions of a few such observables; we give precise results for the backgrounds. These are the first lattice QCD predictions of any quantity along the freezeout curve of heavy-ion collisions. Any non-monotonic behaviour over these is a signal for the critical point; and the lattice results near the critical point do show such behaviour.

Twenty years ago it became clear that QCD has no finite temperature ( $T$ ) phase transition [1], since all quarks are massive, as evidenced by a non-vanishing pion mass. Lattice computations showed that there remained a fairly abrupt change in thermodynamic properties which could possibly influence the physics observed at the RHIC and LHC. About a decade back it was realized that QCD could nevertheless have a critical point at finite baryon chemical potential ( $\mu_B$ ) [2]. There is evidence for such a critical point from modern lattice computations with two light dynamical flavours [3, 4], and from an earlier small volume computation [5]. The behaviour of QCD with two light and a single heavier flavour is not yet settled, although evidence for a critical point is mounting [6].

One question of interest is whether this critical point can be found in experiment. The results of [3, 4] suggest that heavy-ion collision experiments at moderate colliding energies, achievable at RHIC, FAIR and NICA could find it. In these collisions of heavy-ions, a fireball is created which evolves chemically and thermally before freezing out. The primary question of experimental interest is how close the freezeout is to the critical point. In this work we employ Padé resummation of lattice results to obtain predictions which can be directly compared with experiments.

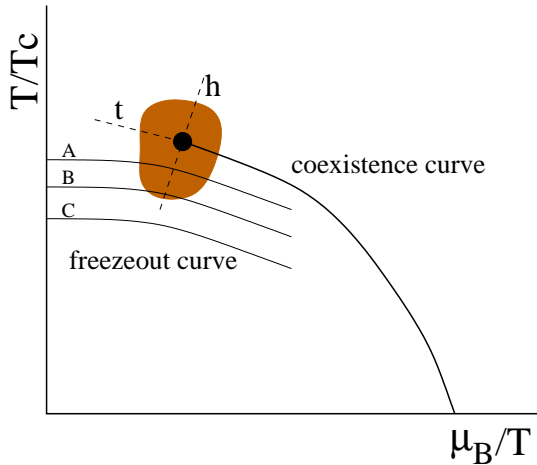


FIG. 1: The critical point of QCD is the end point of a line of coexistence of two phases. One of the interesting questions for heavy-ion physics is how close the freezeout curve is to the critical point, *i.e.*, which of the three is the true position of the freezeout curve. Our results, discussed below, show that  $T_c = 170$  corresponds to a line like A, whereas an increase of 5 to 10 MeV in  $T_c$  could shift the results to the curve C.

There has been some discussion on suitable observables for the identification of a critical point. The first suggestion was to study the width of the distribution of event-by-event (E/E) observations of momenta of particles [2]. Later it was realized that a measurement which was suggested in a different context could be suitable: that of the width of E/E distributions of conserved quantities [7]. For the baryon number, this is proportional to the baryon number susceptibility (BNS) [8, 9], and is expected to diverge in a thermodynamically large sample in equilibrium at the critical point. It was soon pointed out that non-linear susceptibilities (NLS) have stronger divergence [3, 10]. As a result, higher cumulants of the E/E distributions are also good signals for the critical point [11, 12]. It has been pointed out recently that ratios of cumulants are better [13], since ill-determined parameters such as the fireball volume do not appear, and they are directly comparable to predictions from lattice QCD—

$$m_1 = \frac{T\chi^{(3)}(T, \mu_B)}{\chi^{(2)}(T, \mu_B)}, \quad m_2 = \frac{T^2\chi^{(4)}(T, \mu_B)}{\chi^{(2)}(T, \mu_B)}, \quad m_3 = \frac{T\chi^{(4)}(T, \mu_B)}{\chi^{(3)}(T, \mu_B)}, \quad (1)$$

where  $\chi^{(n)}(T, \mu_B)$  is the  $n$ -th order NLS, obtained by taking the  $n$ -th derivative of the pressure with respect to  $\mu_B$ . As one can see, the ratios are not all independent, since  $m_2 = m_1 m_3$ . These ratios are also of interest in lattice studies of the phase diagram of QCD, since they provide estimates of the distance to the nearest singularity of the free energy.

At the critical point,  $(T^E, \mu_B^E)$ , the BNS,  $\chi^{(2)}(T^E, \mu_B^E)$ , diverges. Since this critical point is in the Ising universality class, the eigendirections of the renormalization group scaling transformations can be classified as a “thermal” direction  $t$  and a “magnetic” direction  $h$ , as illustrated in Figure 1. The baryon-baryon correlation length diverges with exponent  $y_t$  as one approaches the critical point in the direction  $t$ , and with exponent  $y_h$  along  $h$ . Once these exponents are known, the divergence of the BNS can be worked out. In the present work we do not need the value of the exponent  $\delta$ , which controls the divergence of the baryon number susceptibility through  $\chi^{(2)}(\mu_B) \simeq |\mu_B - \mu_B^E|^\delta$ . All we need to know is that

$$\chi^{(n)} \simeq |\mu_B - \mu_B^E|^{\delta+n-2}. \quad (2)$$

As a result, the ratios of successive NLS diverge as  $1/|\mu_B - \mu_B^E|$  as one approaches the critical end point. Due to the CP symmetry of QCD, a critical point at  $\mu_B^E$  implies another at  $-\mu_B^E$  with the same critical exponents. Hence, the divergence of the ratios of successive NLS can be rewritten as  $1/|\mu_B^2 - (\mu_B^E)^2|$ .

In lattice calculations one uses the Maclaurin series expansion of the BNS,

$$\frac{\chi^{(2)}(T, z)}{T^2} = \frac{\chi^{(2)}(T)}{T^2} + \frac{1}{2!}\chi^{(4)}(T)z^2 + \frac{1}{4!}T^2\chi^{(6)}(T)z^4 + \frac{1}{6!}T^4\chi^{(8)}(T)z^6 + \mathcal{O}(z^8), \quad (3)$$

organized as an expansion in the dimensionless quantity  $z = \mu_B/T$  at fixed  $T$ . The Taylor (Maclaurin) coefficients,  $T^{n-4}\chi^{(n)}(T)$ , which are also dimensionless, are evaluated through lattice computations at  $\mu_B = 0$ . We have written the expansion out to the order up to which the coefficients are currently known [3, 4]. The successive estimators of the radius of convergence of this series are

$$r_{n,n+2}^2 = (n+2)(n+1)\frac{\chi^{(n)}(T)}{T^2\chi^{(n+2)}(T)}. \quad (4)$$

These have been used to estimate the position of the critical point in [3, 4], where the finite volume effects in these ratios were investigated. It was found that  $r_{n,n+2}^2$  for  $n \leq 6$  were insensitive to the volume, provided  $V \geq (4/T)^3$ .

In terms of these quantities the expansion of eq. (3) can be written as

$$\frac{\chi^{(2)}(T, z)}{T^2} = \frac{\chi^{(2)}(T)}{T^2} \left[ 1 + \frac{z^2}{r_{24}^2} + \frac{z^4}{r_{24}^2 r_{46}^2} + \frac{z^6}{r_{24}^2 r_{46}^2 r_{68}^2} + \mathcal{O}(z^8) \right], \quad (5)$$

Clearly, the ratios of eq. (1) depend only on the three quantities  $r_{24}^2$ ,  $r_{46}^2$  and  $r_{68}^2$ , and not on  $\chi^{(2)}(T)$ . By taking formal derivatives of the expansion above one obtains the higher order susceptibilities. Using these one arrives at the formal series expansions of the measurements we are interested in—

$$\begin{aligned} \frac{1}{z}m_1 &= \frac{2}{r_{24}^2} + z^2 2 \left( \frac{2}{r_{46}^2} - \frac{1}{r_{24}^2} \right) \frac{1}{r_{24}^2} + z^4 2 \left[ \frac{3}{r_{46}^2} \left( \frac{2}{r_{68}^2} - \frac{1}{r_{24}^2} \right) + \frac{1}{r_{24}^4} \right] \frac{1}{r_{24}^2} + \mathcal{O}(z^6), \\ m_2 &= \frac{2}{r_{24}^2} + z^2 2 \left( \frac{6}{r_{46}^2} - \frac{1}{r_{24}^2} \right) \frac{1}{r_{24}^2} + z^4 2 \left[ \frac{1}{r_{46}^2} \left( \frac{15}{r_{68}^2} - \frac{7}{r_{24}^2} \right) + \frac{1}{r_{24}^4} \right] \frac{1}{r_{24}^2} + \mathcal{O}(z^6), \\ zm_3 &= 1 + z^2 \left( \frac{4}{r_{46}^2} \right) + z^4 \left( \frac{3}{r_{68}^2} - \frac{2}{r_{46}^2} \right) \frac{4}{r_{46}^2} + \mathcal{O}(z^6). \end{aligned} \quad (6)$$

It has been demonstrated that series expansions are not a good way to extrapolate physical quantities to finite chemical potential, and better techniques, such as Padé resummations are needed [4]. Since we know that  $m_1$  and  $m_3$  have simple poles and  $m_3$  has a double pole, Padé approximants of appropriate order are particularly suited to this problem—

$$m_1 = z P_1^L(z^2; a, b), \quad m_3 = \frac{1}{z} P_1^L(z^2; a', b'), \quad m_2 = \tilde{P}_2^L(z^2; \tilde{a}, \tilde{b}), \quad (7)$$

where the notation  $P_M^L$  indicates that the numerator is a polynomial of order  $L$  and the denominator is of order  $M$  and  $\tilde{P}_{2M}^L$  indicates that the denominator is the square of a polynomial of order  $M$ . Since we have three terms of each series at our disposal, in each case we can use  $L = 0$  and 1. When longer series expansions become available, one can use larger values of  $L$ . The parameters  $a_0 \dots a_{L-1}$ ,  $a'_0 \dots a'_{L-1}$ , and  $\tilde{a}_0 \dots \tilde{a}_{L-1}$  in the numerator and  $b_1$ ,  $b'_1$  and  $\tilde{b}_1$  in the denominator are obtained by matching to the series expansions [14]. This is done within jack-knife blocks. We check that the relation  $m_2 = m_1 m_3$  is satisfied within errors.

$\sqrt{S_{NN}}$	$z$	$T/T_c$	$\beta(N_t = 6)$	$\beta(N_t = 4)$
5.0	4.7 (2)	0.70 (3)		5.20
7.7	3.02 (1)	0.82 (2)		5.22
11.5	2.08 (7)	0.89 (1)	5.39	5.24?
18.0	1.39 (5)	0.94 (1)	5.41	5.275
19.6	1.29 (4)	0.94 (1)	5.41	5.275
27.0	0.96 (2)	0.96 (1)	5.415	5.275
39.0	0.68 (2)	0.97 (1)	5.415	5.275
62.4	0.44 (2)	0.97 (1)	5.415	5.275
200.0	0.142 (5)	0.98 (1)	5.415	5.275
850.0	0.034 (1)	0.98 (1)	5.415	5.275
2500.0	0.0115 (4)	0.98 (1)	5.415	5.275
5000.0	0.0058 (2)	0.98 (1)	5.415	5.275

TABLE I: The values of  $z = \mu_B/T$  and  $T/T_c$  at freezeout for various  $\sqrt{S_{NN}}$  are shown for  $T_c = 170$  MeV. The numbers in brackets are errors in the least significant digit and come from the statistical error quoted in [15]. There are also statistical errors on the scale setting on the lattice [3, 4]. The combination of these errors may result in the same coupling,  $\beta$ , corresponding to several different central values of  $T/T_c$ . Missing entries for  $\beta$  mean that the simulations in [3, 4] do not correspond to these conditions).

In order to compare lattice predictions with experiment one needs the values of  $T$  and  $\mu_B$  along the freezeout curve as a function of the center of mass energy of the colliding nuclei,  $\sqrt{S_{NN}}$ . These were extracted from data in [15]. For a comparison with lattice computations it is necessary to convert to the dimensionless variables  $z = \mu_B/T$  and  $T/T_c$ . We have used a crossover temperature  $T_c = 170$  MeV consistent with the current best estimates [18, 19]. The correspondences between lattice parameters and the freezeout points are given in Table I, where we have tabulated parameters corresponding to the RHIC low-energy run as well as the LHC heavy-ion runs at both full energy and the expected energy at the end of the current year.

Once all non-thermal sources of fluctuations are eliminated from data, the ratios of eq. (1) are directly comparable to lattice QCD predictions. Lattice predictions have long been used to interpret experimental data from heavy-ion collisions; examples being the qualitative agreement of the equation of state of hot QCD matter with experimentally extracted values and the agreement of strangeness production parameters extracted from lattice measurements and fits to hadron yields. These have been indirect agreements, since a layer of analysis stands between the data and the prediction. The main results of this paper allow direct comparison of lattice predictions and data for these ratios along the freezeout curve. Agreement of data with these values are direct tests of lattice QCD, and could potentially be the first quantitative tests of lattice QCD in a thermal environment. However it is interesting to point out other aspects of this argument.

If the critical point is far from the freezeout curve over a certain range of energy, then  $m_1$  decreases with increasing  $\sqrt{S_{NN}}$  (since  $z$  decreases) and  $m_3$  increases. Using these two measurements and comparing with lattice predictions, it is possible to estimate the freezeout conditions:  $T/T_c$  and  $\mu_B/T$ . This method is independent of the usual one in which hadron yields are interpreted through a resonance gas picture [15]. Comparison of the two methods then allows us to estimate  $T_c$  by inverting the argument of the previous paragraph. Mutual agreement of the values of  $T_c$

so derived at different  $\sqrt{S_{NN}}$  would constitute the first firm experimental proof of thermalization. If this proof holds then one also obtains the simplest and most direct measurement of  $T_c$  found till now. Since such a thermometric measurement can be made reliably with data at large  $\sqrt{S_{NN}}$ , where  $\mu_B$  is small, it would remain a valid measurement whether or not a critical point is found in the low energy scan at RHIC.

Our numerical results are based on the measurements of the Taylor coefficients in the expansion of eq. (3) which were reported in [3, 4]. Since the data were taken at two different series of lattice spacings, with  $N_t = 4$  and 6, one can examine the approach to the continuum limit. In both sets of simulations the pion mass was close to physical, being about 230 MeV. The spatial volume varied from  $(2/T)^3$  to  $(4/T)^3$  at all lattice spacings, and up to  $(6/T)^3$  on the coarser lattice. The present analysis was performed using a jack-knife estimator of the mean and its error with 5–10 jack-knife blocks. We used only statistically independent measurements, of which we have more than 50 at each coupling and volume.

A test of the method is to use it at the previously determined value of  $T^E/T_c$  and check whether the extrapolations give radii of convergence which are compatible with that previous estimate. The Taylor expansion of  $\chi^{(2)}$  around  $z_0 = \mu_B^0/T$  is

$$\frac{\chi^{(2)}(T, z)}{T^2} = \frac{\chi^{(2)}(T, z_0)}{T^2} + \frac{\chi^{(3)}(T, z_0)}{T}(z - z_0) + \frac{\chi^{(4)}(T, z_0)}{2!}(z - z_0)^2 + \mathcal{O}((z - z_0)^3). \quad (8)$$

This implies that  $1/m_1$  and  $2/m_3$  are estimates of the radii of convergence of the series. When they are computed at  $T^E$  then  $z_0 + 1/m_1$  and  $z_0 + 2/m_3$  have to be compatible with previous estimates of  $\mu^E/T^E$ , obtained from the Maclaurin expansion of eq. (5). We have verified this for both  $N_t = 4$  and 6.

This argument also allows us to understand systematics due to lattice volume effects and finite lattice spacing, and, therefore, the possible effects of improved actions. Away from the vicinity of the critical point finite volume effects are expected to be small as long as  $VT^3 \geq 4^3$ . Finite volume effects are expected to be larger near the critical point: indeed this is one way to check whether lattice extrapolations show genuine critical effects. Lattice spacing effects are also easy to understand. Since the Maclaurin series for  $zm_3$  starts with unity, lattice spacing correction are expected to be negligible and small. Indeed, this is what is observed. On the other hand, since the Maclaurin series for  $m_1/z$  and  $m_2$  start with the terms  $\chi^{(4)}(T)/\chi^{(2)}(T)$ , one expects that a large part of these lattice effects can be subsumed into the lattice spacing effects on these quantities. We can correct for the lattice spacing changes between  $N_t = 4$  and 6 using data from [3, 4]. However, there is not yet enough data to extrapolate to the continuum. Note however, that  $m_1/z$  and  $m_2$  have a common normalization. Hence we normalize to  $m_2 = 1$  at  $\sqrt{S_{NN}} = 5$  TeV.

With these normalizations, we find that at freezeout in the highest RHIC energy of  $\sqrt{S_{NN}} = 200$  GeV

$$m_1 = 0.140 \pm 0.008, \quad m_2 = 0.95 \pm 0.06, \quad m_3 = 6.99 \pm 0.06. \quad (9)$$

The errors shown are purely statistical. The remaining systematic error comes from the imprecision in our current knowledge of  $T_c$ . We can estimate the magnitude of this systematic error by changing  $T_c$  by 5 MeV. For example, using  $T_c = 175$  we find, using the corresponding normalization, that

$$m_1 = 0.14 \pm 0.01, \quad m_2 = 1.04 \pm 0.07, \quad m_3 = 7.3 \pm 0.1. \quad (10)$$

Hence this source of uncertainty changes results by less than 10% at the highest RHIC energy. Closer to the critical region the changes can be much larger. For instance, whether  $m_2$  and  $m_3$  are negative at some  $\sqrt{S_{NN}}$ , as seen in Figure 2, depends sensitively on the choice of  $T_c$ —not being visible for the higher value of  $T_c$ .

The dependence of  $m_1$ ,  $m_2$  and  $m_3$  on the energy,  $\sqrt{S_{NN}}$ , along the freezeout curve is shown in Figure 2. Note that the lattice spacing dependence is under good control for  $\sqrt{S_{NN}} > 50$  GeV. In this region of energies  $z = \mu_B/T$  is small, as a result of which the Padé approximants are almost constant and one has  $m_1 \simeq z$ ,  $m_2 \simeq 1/z$  and  $m_3 \simeq z^0$ . Since the freezeout temperature here is smaller than  $T_c$ , one should compare our results with the predictions of resonance gas models. These give  $m_2 = 1$  [16, 17], which is close to our results. In our normalization an ideal quark gas yields  $m_2 = 2/(3\pi^2)$ , which is very different.

In the region of energy just below  $\sqrt{S_{NN}} = 50$  GeV the lattice spacing dependence of the results is not under good control yet. This is related to the fact that the critical point observed on the lattice [3, 4] lies in this region and shifts with the lattice spacings used. Due to this shift in the critical point with lattice spacing, the two lattice spacings give different predictions in this region. As mentioned above, the choice of  $T_c$  is also important. In order to show the expected behaviour near the critical point, we have also shown the results for a single lattice spacing—the smallest currently available. Note that the behaviour of  $m_1$  is fairly smooth, although a departure from the behaviour  $m_1 \simeq z$  is clear. Both  $m_2$  and  $m_3$  show signs of non-monotonic behaviour with the Kurtosis becoming negative. Such

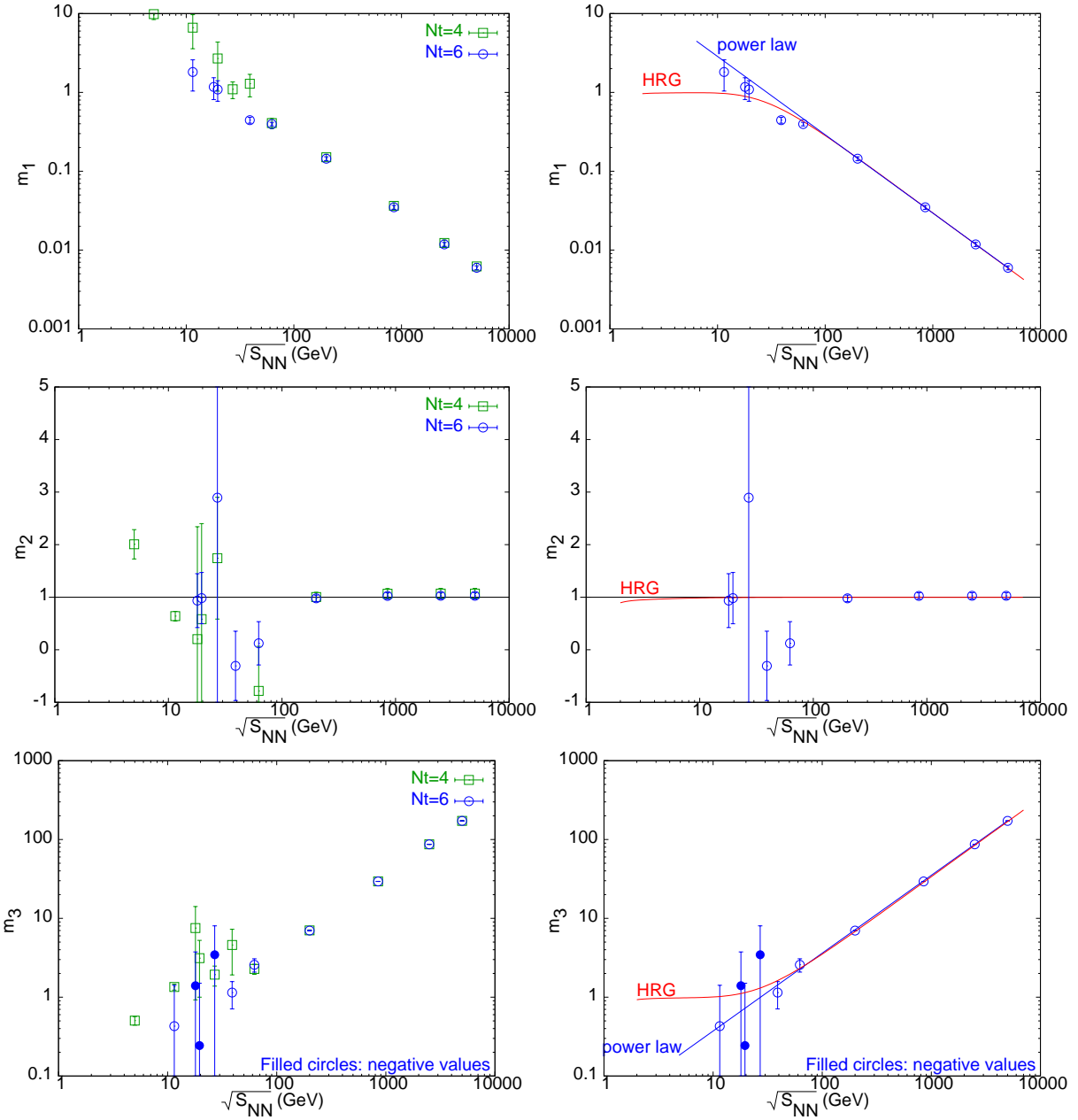


FIG. 2: The ratios  $m_1$ ,  $m_2$  and  $m_3$  along the freeze out curve as a function of  $\sqrt{S_{NN}}$ . The panels on the left compare the lattice results for  $N_t = 4$  and 6. Those on the right show only  $N_t = 6$  along with the hadron resonance gas results [16], marked HRG, and a simple power law extrapolation of high-energy data, in order to make clearer the non-monotonicity near the critical region.

leptokurtic behaviour is impossible in the hadron resonance gas. It develops in QCD only when the lattice spacing is small enough.

At very small  $\sqrt{S_{NN}}$  one again leaves the vicinity of the critical point, and the lattice spacing effects are again under reasonable control. This happens although  $z = \mu_B/T$  is very much larger than unity, and the lattice measurements, made at  $z = 0$ , have to be extrapolated very far. The reliability of the lattice prediction at large  $z$  is due to the stability of the Padé resummations. Note that in this region there is a return to the expected behaviour  $m_1 \simeq z$ ,  $m_2 \simeq 1/z$  and  $m_3 \simeq z^0$ .

Since thermodynamic stability requires  $\chi^{(2)}$  to be positive, the signs of  $m_1$  and  $m_2$  immediately tell us the signs of both  $\chi^{(3)}$  and  $\chi^{(4)}$ . Our observations then show that  $\chi^{(3)}$  is positive along the freezeout curve, in agreement with the

qualitative argument of [12]. This implies that those parts of the freezeout curve which current lattice computations can access lie entirely below the line of first-order transitions. It is a moot question whether the freezeout line crosses the first-order line (*i.e.*, the coexistence line of Figure 1) at lower energies or whether future lattice computations at smaller lattice spacings will show different behaviour.

The most pleasant aspect of the current results is that the critical point is close enough to the freezeout curve for its effect to be visible as non-monotonic behaviour of the ratios. This is clearest for  $m_1$  because of the relatively smaller error bars. However, the effect is also present in  $m_2$  and  $m_3$ . There is currently some uncertainty in the position and size of the peak due to uncertainties in lattice determinations of  $T_c$ . However, all the available lattice data show that the critical point lies within reach of the proposed energy scan at the RHIC. We emphasize that the existence of non-monotonicity is a general expectation if there is a nearby critical point. The baseline over which the behaviour stands is a precise result from lattice QCD which is new.

In this letter we have examined lattice QCD predictions for the ratios in eq. (1). On the lattice they are related to the radius of convergence of the series in eq. (8), and they are also measurable in experiments [13]. Using Padé approximants to resum the series expansion of these ratios (which reproduce previous results on the location of the critical point) we predict the ratios along the freezeout curve (see Figure 2). Current lattice results already show the following important qualitative and quantitative trends—

1. Generally  $m_1$  decreases with increasing  $\sqrt{S_{NN}}$  and  $m_3$  increases, whereas  $m_2$  has a flatter dependence on energy. This general trend is interrupted in the neighbourhood of a critical point where there are rapid and non-monotonic changes in all three observables.
2. At the highest energies (RHIC and LHC) sufficiently accurate measurements of  $m_1$  and  $m_3$  may be used to deduce the value of the crossover temperature,  $T_c$ .
3. The skew and kurtosis are both expected to be positive in the range of energies away from the critical point, with a possible change in the sign of the kurtosis in the critical region.

These computations were performed on the Cray X1 of the ILGTI at TIFR. RVG would like to acknowledge the hospitality of the Department of Physics at the University of Bielefeld. SG would like to thank Bedangadas Mohanty and Nu Xu for discussions. We would like to thank Sandeep Chatterjee for tables of  $m_1$ ,  $m_2$  and  $m_3$  along the freezeout curve in the hadron resonance gas model.

\* Electronic address: gavai@tifr.res.in

† Electronic address: sgupta@tifr.res.in

- [1] F. Karsch, *Nucl. Phys. Proc. Suppl.* 15 (1990) 157; A. Ukawa, *Nucl. Phys. Proc. Suppl.* 17 (1990) 118; F. R. Brown *et al.*, *Phys. Rev. Lett.* 65 (1990) 2491.
- [2] M. A. Stephanov, K. Rajagopal, E. V. Shuryak, *Phys. Rev.* , D 60, 114028, (1999).
- [3] R. V. Gavai and S. Gupta, *Phys. Rev.* D 71, 114014 (2005).
- [4] R. V. Gavai and S. Gupta, *Phys. Rev.* D 78, 114503 (2008).
- [5] Z. Fodor and S. D. Katz, *J. H. E. P.* 0404, 050 (2004).
- [6] O. Philipsen, arXiv:0910.0785.
- [7] M. Asakawa, U. Heinz and B. Muller, *Phys. Rev. Lett.* 85, 2072 (2000); S.-Y. Jeon and V. Koch, *Phys. Rev. Lett.* 85, 2076 (2000).
- [8] S. Gottlieb *et al.*, *Phys. Rev. Lett.* 59, 2247 (1987).
- [9] R. V. Gavai, *et al.*, *Phys. Rev.* D 65, 054506, (2002); C. Bernard, *et al.*, *Phys. Rev.* D 77, 014503, (2008); M. Cheng, *et al.*, *Phys. Rev.* D 79, 074505, (2009).
- [10] R. V. Gavai and S. Gupta, *Phys. Rev.* D 70, 054006, (2005); C. R. Allton *et al.*, *Phys. Rev.* D 71, 054508, (2005).
- [11] T. Nayak (STAR Collaboration), *Nucl. Phys.* A 830, 555c, (2009); B. Mohanty, *Nucl. Phys.* A 830, 899c, (2009).
- [12] B. Berdnikov and K. Rajagopal, *Phys. Rev.* , D 61 (2000) 105017; S. Ejiri, F. Karsch and K. Redlich, *Phys. Lett.* , B 633 (2006) 275; M. A. Stephanov, *Phys. Rev. Lett.* , 102 (2009) 032301; M. Asakawa *et al.*, *Phys. Rev. Lett.* 103 (2009) 262301.
- [13] S. Gupta, arXiv:0909.4630.
- [14] G. A. Baker and P. Graves-Morris, *Encyclopedia of Mathematics: Padé Approximants*, Vol 13, Part 1, Addison-Wesley Publishing Company, Reading, Massachusetts, (1981).
- [15] A. Andronic, P. Braun-Munzinger and J. Stachel, *Phys. Lett.* , B 673 (2009) 142; H. Oeschler, J. Cleymans, K. Redlich, S. Wheaton, arXiv:0910.2128.
- [16] S. Chatterjee, R. M. Godbole and S. Gupta, *Phys. Rev.* , C 81 (2010) 044907.
- [17] M. Cheng *et al.*, *Phys. Rev.* , D 79 (2009) 074505;

- [18] M. Cheng (HOTQCD collaboration), talk given at the “Strong Interactions in the 21st Century” workshop, Mumbai, February 2010. F. Karsch (HOTQCD collaboration), talk given at the “New Frontiers in QCD” worskop, Kyoto, March 2010.
- [19] Y. Aoki *et al.*, *J. H. E. P.* , 0906 (2009) 088.